MagGrid: Non-Levitative Electromagnet Robot Propulsion Method for 2-D Material Handling

Shangqiu (David) Li

Images/figures created by student unless otherwise referenced

Background

Autonomous Mobile Robots (AMR) swarms:

- ➢Widely used in smart warehouses, sorting centers and manufacturing to bring operational flexibility.
- ➢Market scale up to $18.9 billion by 2032 [1]

However, for high-volume applications involving many AMRs (e.g. grocery packing >2300 robots):

1. <u>Lower productivity</u> from intensive inter-robot coordination and battery charging downtime. [2],[3]
2. High individual complexity requiring many onboard subsystems (locomotion, battery, wireless communication, localization, navigation) causing <u>high system cost and complexity</u> [4],[5]
3. Use of many batteries <u>not environmentally friendly</u>

Image taken from https://www.ocadogroup.com/

Fig. 1. grocery AMR sortation system

Image taken from https://www.bastiansolutions.com/blog/sorting-through-sorters-your-guide-to-sortation-conveyor/

Fig. 2. Package AMR sortation system

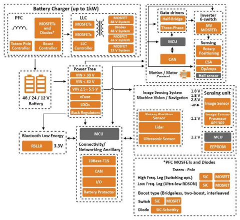

Image taken from https://www.digikey.com/en/product-highlight/o/on-semi/autonomous-mobile-robot

Fig. 3. AMR system diagram

Alternative Solution: <u>Maglev 2D Robots</u>

Dense and costly electromagnet grid, only designed for small operation area usage and ultra-fine precision applications (e.g. photolithography for semiconductors) [6],[7]

Image taken from https://www.pi-usa.us/en/products/precision-motorized-linear-stages/integrated-xy-precision-motorized-stages-planar-xy-stages

Fig. 4. Maglev 2D robot system

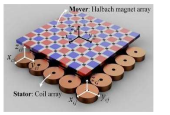

Image taken from: https://doi.org/10.1016/j.matdes.2023.111945

Fig. 5. Maglev 2D robot layout

<u>Gap:</u> Lack of scalable propulsion technology for high-volume operations in 2D material handling

Engineering Objectives

Engineering Need:

Improve fleet-size scalability of existing robot technology and address the gap.

Engineering Goal:

Develop a <u>passive</u> robot propulsion method for high-volume material handling, such that the robots are <u>not powered</u>, and instead controlled and powered by the table/floor.

Compared to AMR swarm:

1. Passive robot swarm is <u>less complex and more cost-effective</u> per robot eliminating the need for battery and various onboard subsystems.
2. Centralized localization, logic and processing for <u>more efficient coordination</u>.
3. Removing battery usage <u>eliminates battery charging downtime and improves sustainability</u>.

Challenges:

1. <u>Robot system architecture</u>: modular, reconfigurable, and expandable
2. <u>Custom mathematical modelling</u>: dynamics (forces and torques) characterization and solving for electromagnet current
3. <u>Robot motion control</u>: integrated and high-speed robot localization, robot motion controller

Methodology

System Architecture

Overall Layout

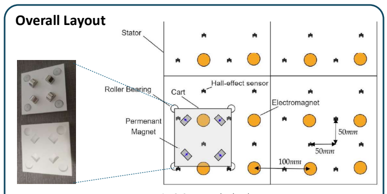

Fig. 6. Stator and robot layout

- Robots are made up of four magnets and ball bearings.
- Sparse electromagnet (EM) grid for propulsion
- Hall-effect sensors (HE) sense magnetic field of robot for localization
- Stator system (electromagnet and Hall-effect sensor system) is 400mm x 300mm.
- Split into 100mm x 100mm stator modules

Various expansion and reconfiguration:

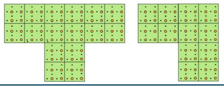

Fig. 7.

I2C communication:

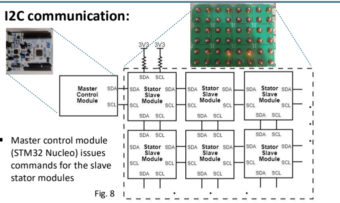

- Master control module (STM32 Nucleo) issues commands for the slave stator modules

Fig. 8

Implementation

Hardware:

- Onboard microcontroller (STM32F103) controls electromagnets and reads Hall-effect sensors (Fig.9)
- Stacked design with the Hall-effect sensors on top PCB and the main control circuitry on the bottom PCB, connected with pin headers. The two PCBs are aligned and secured with standoffs. Electromagnets are supported by 3D-printed fixture.(Fig.10)
- Custom PCB design for stator modules (Fig.11)

Software

- Implemented using embedded C and FreeRTOS
- Responds to master control module as I2C slave to respond with Hall-effect values read by ADC and receives PWM value for H-bridge (Fig.12)

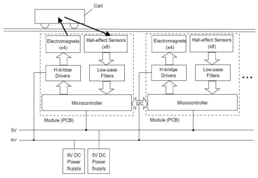

Fig. 9. Stator modules block diagram

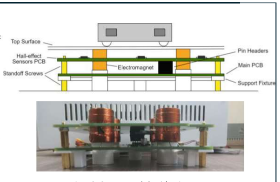

Fig. 10. Stator module side view

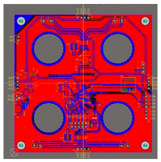

Image created with Altium Designer tool (altinum.com)

Fig. 11. Main PCB custom design

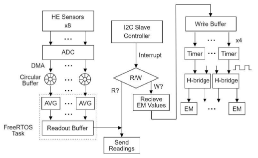

Fig. 12. Stator module software

Motion Control Modelling

Localization

Location

Position => Sensor Reading:

Radial magnetic field of a cylindrical magnet:

$$ {}^{b}B_{\rho} = -\frac{B_r}{4\pi}\int_0^{2\pi}\int_0^{a}\left(-\frac{R(2^{b}\rho - 2R\cos\varphi)}{2\left(R^2+(L/2-z)^2+{}^{b}\rho^2-2R^{b}\rho\cos\varphi\right)^{3/2}}+\frac{R(2\rho-2R\cos\varphi)}{2\left(R^2+\left(L/2+{}^{b}z\right)^2+{}^{b}\rho^2-2R^{b}\rho\cos\varphi\right)^{3/2}}\right)dRd\varphi $$

Superposition principle for magnetic field of all four magnets (Fig.13 (a))

Sensor Reading => Position:

- ➢ Possible robot locations given a sensor reading:
  Level set of robot magnetic field (Fig.13 (b))
- ➢ Transform to probability density distribution (PDF):
  Overlaying 2D Gaussian distribution to level set (Fig. 14 (a))
- ➢ Incorporating multiple sensor readings:
  Average of sensor PDFs (mixed probability distribution) (Fig. 14.(b))

Fig. 13

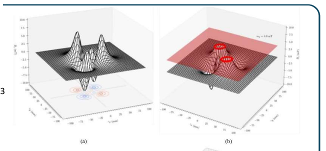

(a) (b)

Fig. 14

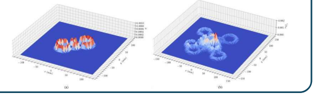

(a) (b)

Dynamics Modeling

Force coefficients (current vs. forces)

1. Electromagnet approximation as an ideal dipole (linear with current) (Fig. 15)
2. Derived force & torque relationships with current (force linear coefficients F_s & τ_s) (Fig. 16)

$$ \vec{F} = \nabla({}^{m}\vec{m}\cdot{}^{c}B_z({}^{c}\vec{p}_d)) \qquad \vec{\tau} = I\,k_i\left[-{}^{c}B_y({}^{c}\vec{p}_d),\ {}^{c}B_x({}^{c}\vec{p}_d),\ 0\right]^T $$

$$ \vec{F} = F_s({}^{m}\vec{p}_d)\mathrm{I} \qquad \tau = \tau_s({}^{m}\vec{p}_d)\mathrm{I} $$

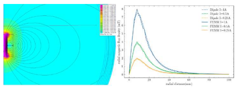

Image left created with Finite Element Method Magnetics (femm.info)

Fig. 15

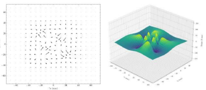

Fig. 16

Decoupling

Electromagnet currents

- ➢ Allows for decoupled (independent) control of three degree of freedom (F_x, F_y, τ)

Variables:

Target wrench vector: $\overrightarrow{W} = [F_x, F_y, \tau]^T$

Force coefficients: $K(\vec{p}) = \begin{bmatrix} \hat{x}F_{s_1}(\vec{p}) & \hat{x}F_{s_2}(\vec{p}) & \dots & \hat{x}F_{s_n}(\vec{p}) \\ \hat{y}F_{s_1}(\vec{p}) & \hat{y}F_{s_2}(\vec{p}) & \dots & \hat{y}F_{s_n}(\vec{p}) \\ \tau_{s_1}(\vec{p}) & \tau_{s_2}(\vec{p}) & \dots & \tau_{s_n}(\vec{p}) \end{bmatrix}$

Electromagnet currents: $\vec{\imath} = [i_1, i_2 \dots i_n]^T$

Relationships:

$\overrightarrow{W} = K({}^{m}\vec{p}_d)\vec{\imath}$ solve for current => $\vec{\imath} = K^{-1}({}^{m}\vec{p}_d)\overrightarrow{W}$

where K^{-1} is the pseudoinverse (least squared).

Complete Control Loop

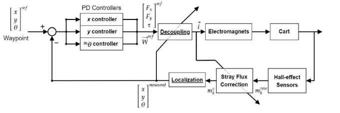

Fig. 17

1. PD controllers give target forces and torque for target waypoint
2. Decoupling converts it into necessary EM currents using results from localization and dynamics modelling
3. Localization takes corrected HE readings and give robot feedback to the PD controllers

- Localization is performed on the Teensy 4.0, the rest is on the Nucleo.
- Teensy 4.0 is queried by the Nucleo via SPI.
- The entire control loops runs at ~400Hz.

Prototype/Validation

Prototype:

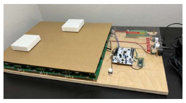

Fig. 18

Localization Testing:

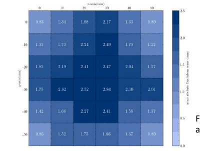

Average Euclidean distance error: 1.785mm (SD: 0.77mm, N=36*1000)

Fig. 19. Localization errors at various locations

Movement Trials:

Various motion trials:

Tested four motion types: spinning in place, straight line, corner, square.

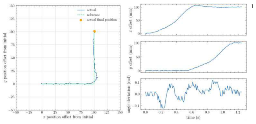

Fig. 20. Corner motion

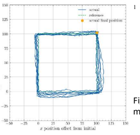

Fig. 21. Square motion

General characteristics

Table 1

Characteristic	Value
Max. Acceleration	8.63 m/s²
Max. Velocity	1.31 m/s
Max. Angular Acceleration	2979 deg/s²
Max. Angular Velocity	2165 deg/s (360.8 RPM)
Max. Load	~ 500 g
Mean Absolute Tracking Error	3.2 mm[1]
Mean Absolute Positioning Error	1.2 mm[1]
Power Consumption	Max. 40.5 W

N=10, straight motion at 300mm

[1] ±0.77 mm

Discussion/Conclusion

Innovations:

- **Key Idea:** This research for the first time proposes a wheeled robot propulsion method of non-levitative electromagnet propulsion to shift the existing self-propelled propulsion paradigm into a table/floor-propelled.
- **Innovation:** This research presents new magnet layouts (<u>~20x less copper vs. maglev robots)</u>, expandible stator system architecture, and custom mathematical modeling.
- **Proof:** The viability of this method has been verified by the developed prototype and experiment (3.2mm mean absolute tracking error)

Impact:

- **Application:** This method can be applied to many industrial material handling tasks (e.g. parcel sorting, product assembly line, enclosure manufacturing).

Future work:

- Extend the propulsion carrying capacity to be integrated for real world applications with higher power
- Explore and optimize electromagnet layout and shapes
- Other applications such as assistive automobile propulsion on highways

References

[1] "Autonomous Mobile Robot Market Size, Share, Competitive Landscape and Trend Analysis Report by Type, By Application, By End User : Global Opportunity Analysis and Industry Forecast, 2022-2032," Allied Market Research, May 2023.

[2] Chowdhary, R. R., Chattopadhyay, M. K., & Kamal, R. (2021). Comparative study of orchestrated, centralised and decentralised approaches for orchestrator based task allocation and collision avoidance using network controlled robots. Mağalaẗ Ğam'aẗ Al-malīk Saud : Ùlm Al-ḥasib Wa Al-ma'lumat, 33(10), 1231–1241. https://doi.org/10.1016/j.jksuci.2018.09.001

[3] Kundu, T., & Saha, I. (2018). Charging Station Placement for Indoor Robotic Applications. 2018 IEEE International Conference on Robotics and Automation (ICRA). https://doi.org/10.1109/icra.2018.8461006

[4] P.-E. Dossou, P. Torregrossa, and T. Martinez, "Industry 4.0 concepts and lean manufacturing implementation for optimizing a company logistics flows," Procedia Comput Sci, vol. 200, pp. 358–367, 2022, doi: 10.1016/j.procs.2022.01.234.

[5] Siegwart, R., Nourbakhsh, I. R., & Scaramuzza, D. (2011). Introduction to autonomous mobile robots. MIT press.

[6] H. Fu, C. Hu, M. Zhang, and Y. Zhu, "Integrated optimization of 3D structural topology and 2D Halbach parameters for maglev planar motor," Mater Des, vol. 230, p. 111945, Jun. 2023, doi: 10.1016/j.matdes.2023.111945.

[7] H. Zhu, T. J. Teo, and C. K. Pang, "Design and Modeling of a Six-Degree-of-Freedom Magnetically Levitated Positioner Using Square Coils and 1-D Halbach Arrays," IEEE Transactions on Industrial Electronics, vol. 64, no. 1, pp. 440–450, Jan. 2017, doi: 10.1109/TIE.2016.2598811.